Senile plaques in Alzheimer's disease are primarily induced by cerebral vessel leakage of red blood cells and other blood contents

Hualin Fu[1, 2*], Jilong Li[1], Peng Du[3], Weilin Jin[1, 2], Daxiang Cui[1, 2]

Affiliations:

[1] Institute of Nano Biomedicine and Engineering, Department of Instrument Science and Engineering, School of Electronic Information and Electrical Engineering, Shanghai Jiao Tong University, 800 Dongchuan Road, Shanghai, 200240, P. R. China

[2] National Center for Translational Medicine, Shanghai Jiao Tong University, 800 Dongchuan Road, Shanghai, 200240, P. R. China

[3] Department of Colorectal Surgery, Xinhua Hospital, School of Medicine, Shanghai Jiao Tong University, Shanghai, China

*Correspondence to: hfu@sjtu.edu.cn or 1010720220@qq.com (Hualin Fu)

Abstract

Senile plaque is one of the most prominent pathological hallmarks of Alzheimer's disease （AD）. However, the mechanism governing the generation of senile plaques remains a mystery. Many researchers believed that senile plaques are derived from neuronal cells, however, there is also strong evidence showing that senile plaques are linked with cerebral microhemorrhage. We analyzed the major neural markers, cerebral blood vessel and blood-related markers in AD brain sections with immunohistochemistry in conjunction with fluorescence imaging and TUNEL assay. We found few colocalizations between neural markers and senile plaque Aβ staining while abundant colocalizations between blood markers such as HBA and ApoE with senile plaque Aβ. Senile plaques also colocalized with a characteristic blue autofluorescence, which is prominently located in the blood stream and associated

with red blood cells. Additionally, senile plaques does not colocalize with blood vessel marker Collagen IV. It appears that Aβ either directly leaks out of damaged blood vessel wall or is transported out of blood vessel through blood vessel microaneurysm. By staining of another marker of cerebral blood vessel LRP1, we could also observe that Aβ directly came out broken blood vessels at the center of dense-core plaques. In AD brain tissues, platelets were found along blood vessel walls and also in senile plaques, thus platelets likely also contribute to senile plaque formation. In summary, we concluded that senile plaques are primarily induced by cerebral vessel leakage of red blood cells and other blood contents.

Introduction

Alzheimer's disease has several important pathological hallmarks such as senile plaques, neurofibillary tangles and cerebral amyloid angiopathy (CAA)[1-4]. Beta amyloid peptide (Aβ) turned out to be a major component in both senile plaques and CAA[5,6]. However, the mechanism governing Aβ generation in senile plaques and the linkage between CAA and senile plaques is still not clear. Most researchers believed that senile plaques are derived from neuronal cells as proposed in amyloid cascade hypothesis[7,8], on the other hand, there is also strong evidence showing that senile plaques are linked with cerebral microhemorrhage[9-16]. We used immunohistchemistry, fluorescence imaging and TUNEL assay to examine the neural, vascular or blood Aβ contribution to senile plaque development. We found that there is a lack of significant direct neural cell Aβ contribution to senile plaques. The true direct source of senile plaque Aβ appears to be Aβ-associated red blood cells that leak out of cerebral blood vessels while CAA is an important intermediate stage during this senile plaque formation process.

Results:

Neural markers colocalized sparsely with senile plaque Aβ staining

If senile plaque Aβ comes from neural cells, theoretically，senile plaque Aβ should colocalize with some neural markers because *in vivo* Aβ does not exist as a single species molecule but rather associates with many other molecules. We checked the expression of neuronal marker MAP2, pan-neural marker αSYN and phos-Tau and astroglial marker GFAP and microglial marker Iba1 in AD brain tissues. In this manuscript, in order to get a broad image of Aβ-related changes during senile plaque development, "Aβ" refer to all peptides containing the "Aβ" peptide sequence, including the precursor protein APP. We found rare colocalizations between senile plaque Aβ with MAP2, αSYN and phos-Tau (Figure 1 (ⅰ-ⅵ)) and some spotty colocalizations of GFAP or Iba1 with senile plaque Aβ (Figure 1 (ⅶ-ⅹ)). It appears that there were relatively more colocalizations between glial cells with Aβ than colocalizations between neuronal cells with Aβ in the senile plaques. However, overall, there is no prominent neural marker colocalization with senile plaque Aβ. Especially, in the center of dense-core senile plaques, there is rarely localization of any of the neural markers that we have checked. The data suggested Aβ from other sources likely form the bulk of Aβ materials in the senile plaques.

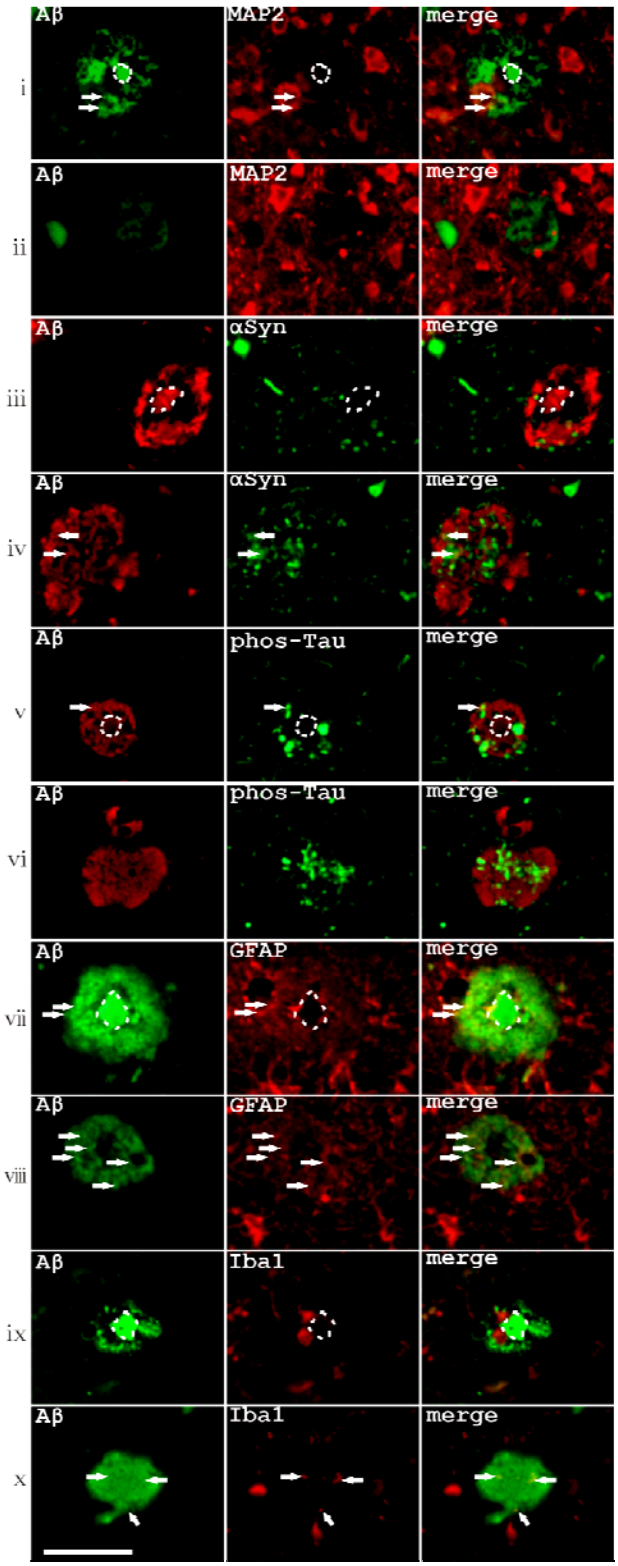

Figure 1. Co-immunostaining of neuronal marker MAP2, pan-neural markers αSYN and phos-Tau or glial cell markers GFAP and Iba1 with Aβ in dense-core or diffusive senile plaques. (i-ii) MAP2; (iii-iv) αSYN; (v-vi) phos-Tau; (vii-viii) GFAP; (ix-x) Iba1. Arrows pointed to colocalizations of markers. The circled areas

indicated the core of dense-core plaques, which rarely colocalized with any of the neural markers examined. Scale bar, 50 μm.

Senile plaque Aβ staining seldom colocalized with nuclear stains

Because Aβ often showed extracellular localizations, people assumed that Aβ might be derived from dead neurons. However, the direct evidence that linked senile plaque Aβ with dying neurons is lacking. In our analysis, most Aβ plaques lacked of nuclei associations, agreeing with their predominantly extracellular localization (Figure 2A). In addition, Aβ plaques did not colocalized with TUNEL-labeled nuclei, disagreeing with the assumption that Aβ might come from dying neurons or dying cells of any kind (Figure 2B). Surprisingly, we observed a faint blue fluorescent staining in the centers of many dense-core plaques, which showed amorphous irregular patterns distinct from densely-stained oval shape nucleus staining (Figure 2A(ii)). To differentiate blue autofluorescence from blue nuclei staining, we switched to use a red fluorescence nuclei dye Propidium Iodide (PI). We proved that the amorphous blue fluorescent staining in the core of senile plaques is a blue autofluorescence specifically associated with senile plaques, but not nuclei staining (Figure 2C). During the process of preparing this manuscript, we noticed that several earlier studies already recognized senile plaques had characteristic autofluorescence although the true source of this blue autofluorescence is unknown[17,18]. To facilitate the study and discussion on this unique and potentially important substance, we would like to give a special name for this material as "MetaBlue" (meaning for a blue metabolite or a mixture of blue metabolites).

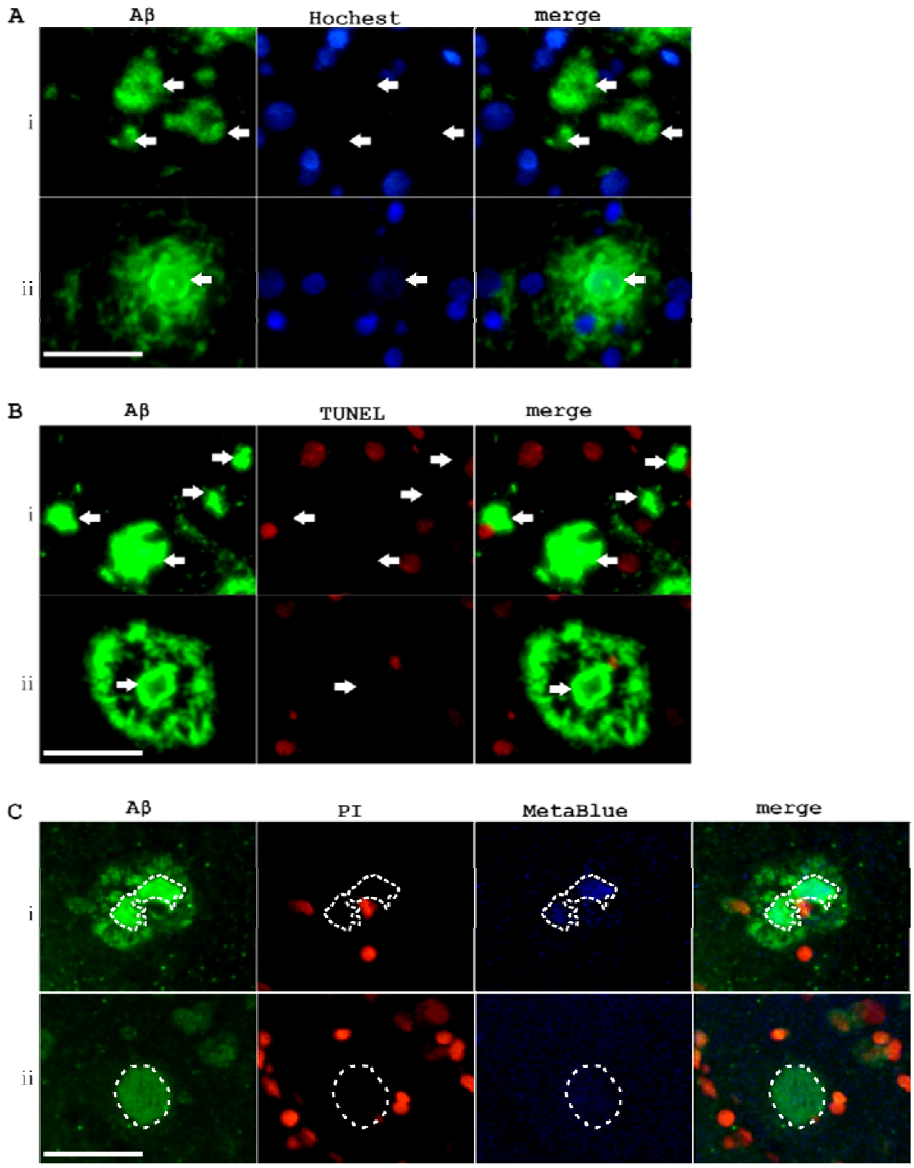

Figure 2. **Senile plaques are seldom associated with nuclei DNA staining. A:** Senile plaques are seldom stained with Hoechst staining. (ⅰ) Diffusive or stella plaques were mostly not stained with Hoechst. (ⅱ) Faint irregular amorphous blue fluorescent signals were observed in condense-core plaques but distinct from nuclear staining. Arrows point to senile plaques. **B**: Diffusive (ⅰ) or dense-core plaques (ⅱ) are not associated with TUNEL-labeled nuclei. Arrows point to senile plaques. **C**: dense core plaques had a relatively strong blue autofluorescence (ⅰ) while the blue autofluorescence signal in diffusive plaques was weak (ⅱ). The dashed lines indicated dense-core or diffusive senile plaques with blue autofluorescence but without PI-positive nuclei. Scale bars, 50 μm.

Senile plaque colocalized with MetaBlue，a specific blue autofluorescence， that is also prominently found in the blood stream.

To trace the origin of MetaBlue, we combined immunohistochemistry staining with autofluorescence imaging. We found that MetaBlue is prominently associated with red blood cells in the blood stream, CAA blood vessel wall and senile plaques (Figure 3). The staining intensity of MetaBlue in the center of dense-core plaques is close to MetaBlue intensity in CAA blood vessels and always higher than in diffusive senile plaques, which suggested that MetaBlue is either degraded or dispersed in diffusive plaques. MetaBlue associated with both Aβ (Figure 3A) and red blood cell marker HBA (Figure 3B) in red blood cells, CAA, dense-core plaques and diffusive plaques. With the senile plaque association of predominantly blood origin MetaBlue， Aβ and red cell marker HBA, it suggested that senile plaque Aβ might directly come from the blood.

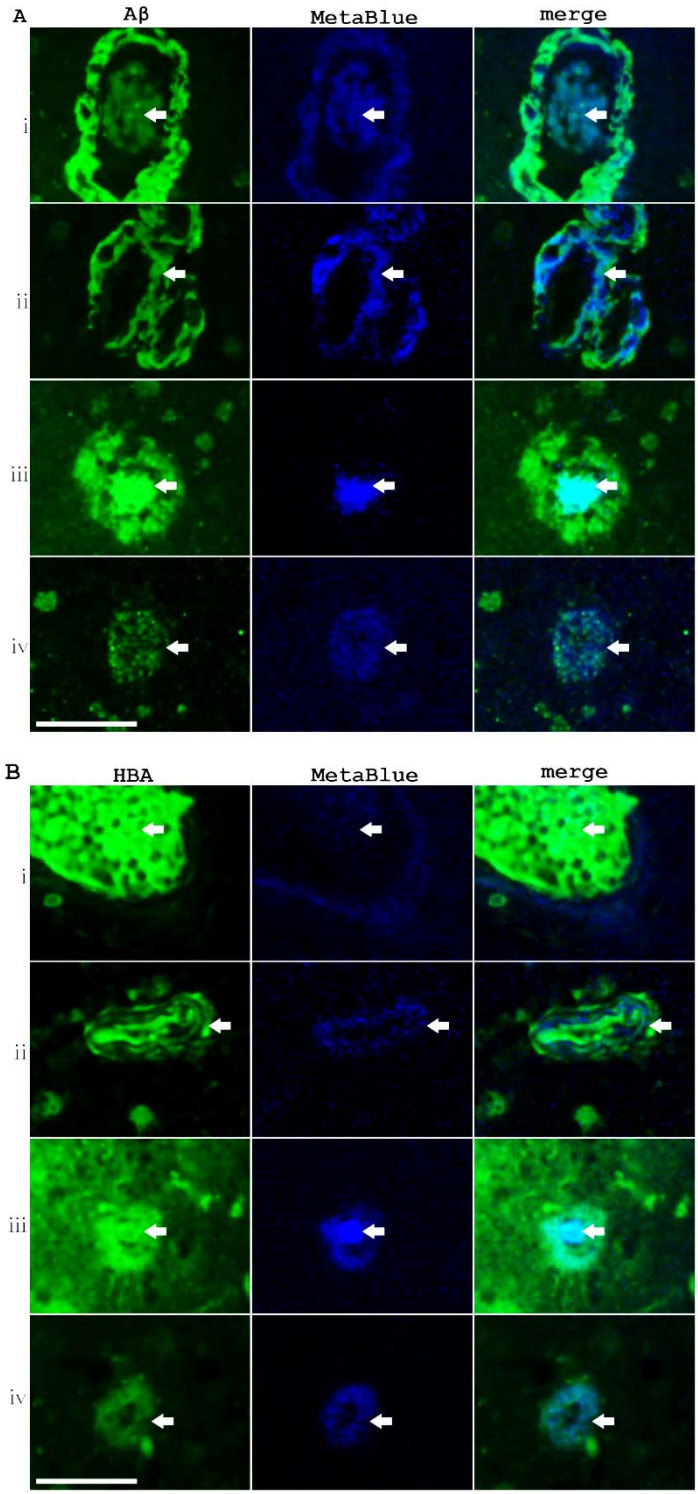

Figure 3. **The MetaBlue blue autofluorescence signals colocalized with Aβ and alpha hemoglobin HBA staining in the red blood cells, CAA, dense-core plaques and diffusive plaques. A**: MetaBlue signals colocalized with Aβ in the red blood cells (i), CAA (ii), dense-core plaques (iii) and diffusive plaques (iv), indicated by

arrows. **B**: MetaBlue signals colocalized with alpha hemoglobin HBA staining in the red blood cells (i) , CAA (ii) , dense-core plaques (iii) and diffusive plaques (iv), indicated by arrows. Scale bars, 50 μm.

Senile plaque Aβ colocalized with blood markers HBA and ApoE

To directly check the association of Aβ with blood markers， we did co-staining of Aβ with blood marker HBA and ApoE. Aβ staining colocalized with HBA in the red blood cells, in the perivascular plaques, in dense-core plaques and in diffusive plaques (Figure 4A). However, in the process of CAA vessel development and perivascular Aβ leakage, some HBA staining does not colocalize with Aβ, with more HBA diffusing away from the blood vessel while most Aβ still retaining on the vessel wall, which suggested that HBA and Aβ leaked out of blood vessel with different speeds (Figure 4A(ii)). More evidence to show that the co-staining of Aβ and HBA in single red cells, in red blood cells with other type of abnormalities than CAA such as blood cell extravasation or intravascular hemolysis in AD tissues was provided in Supplementary Figure 1. Aβ staining also colocalized with ApoE in the perivascular plaques, in dense-core plaques and in diffusive plaques (Figure 4B). However, in relatively normal-looking blood vessels, ApoE was present predominately in the blood plasma and did not associate with Aβ in red blood cells, which suggested that intravascular biochemical events likely happened before the ApoE-Aβ association was formed. We also noticed that ApoE expression was higher in dense-core plaques and its intensity reduced more quickly in diffusive senile plaques comparing to Aβ, which indicated that ApoE and Aβ were metabolized with different rates.

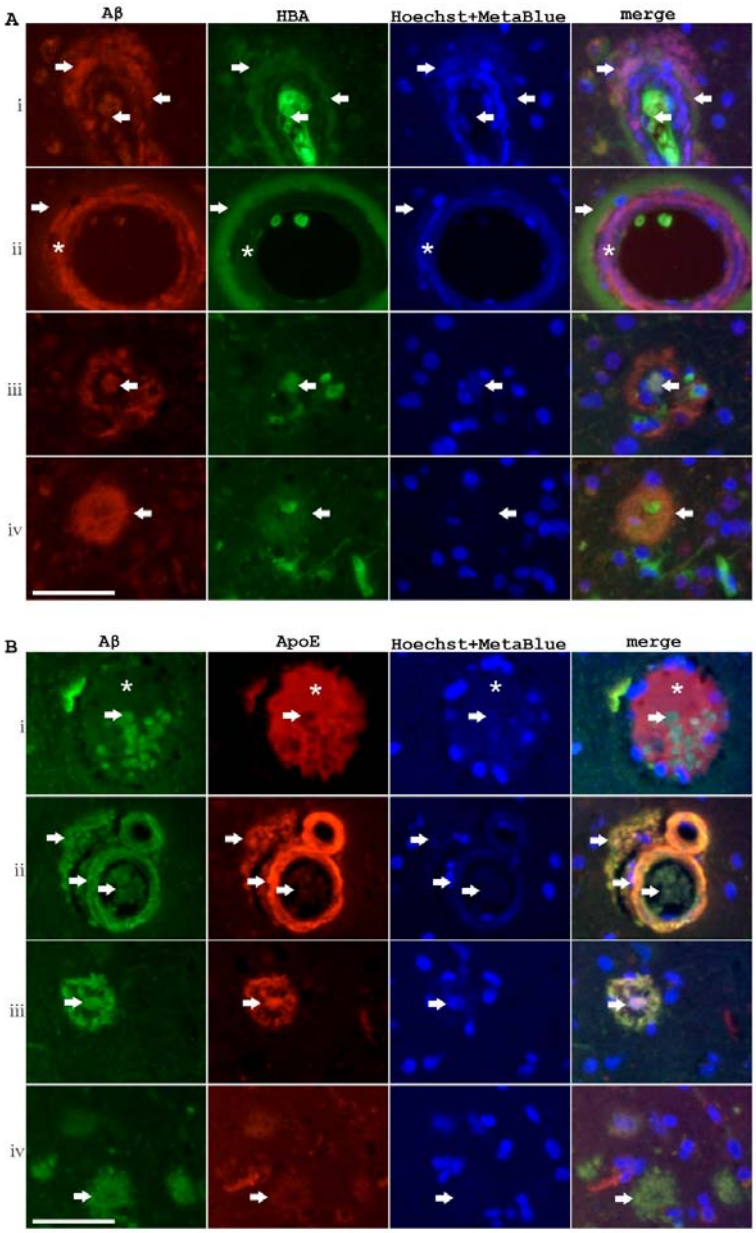

Figure 4. **HBA and ApoE mostly colocalized with Aβ during different stages of senile plaque development but sometimes differently localized. A**: HBA colocalized with Aβ in perivascular plaques (ⅰ), dense-core plaques (ⅲ) and diffusive plaques (ⅳ). However, HBA and Aβ differently localized when diffusing away from CAA blood vessels in (ⅱ). The asterisk indicated a blood vessel. The arrows indicated HBA-Aβ colocalizations. **B**: ApoE mostly colocalized with Aβ in CAA and perivascular plaques (ⅱ), dense-core plaques (ⅲ) and diffusive plaques (ⅳ) however they differently localized in relatively normal looking blood vessels with the majority of ApoE present in the blood plasma while Aβ staining associated

with red blood cells (i). The asterisk indicated the blood plasma. The arrows indicated that Aβ staining often colocalized with ApoE staining. Scale bars, 50 μm.

The dynamic interaction of Aβ expression and blood vessel changes during senile plaque development.

The blood vessels have been long thought to be involved in senile plaque formation[9,10]. However, the exact contribution of blood vessel to senile plaque formation is not so clear. We used ColIV as a blood vessel marker to examine the blood vessel changes during the senile plaque formation process (Figure 5). Firstly, we observed patches of strong Aβ staining in the blood vessel and also in vessel walls in CAA (Figure 5(i-ii)). Secondly, the formation of dense-core plaques and diffusive plaques was associated with blood vessel damages with irregular blood vessel morphology and openings in the blood vessel wall (Figure 5(iii-iv)). Thirdly, the direct leakage of Aβ out of small capillaries and larger blood vessels was observed (Figure 5(v-vi)). In addition, balloon-shape bulge formation in small and large blood vessels was also detected (Figure 5(vii-viii)). These bulges contained condensed staining of Aβ, indicating blood vessel aneurysm could be another way of transporting concentrated Aβ out of blood vessels, which might be the source of Aβ in dense-core senile plaques. This observation is consistent with a previous study stating lumpy and bumpy blood vessels were found in AD brain tissues by using scanning electron microscopy[19].

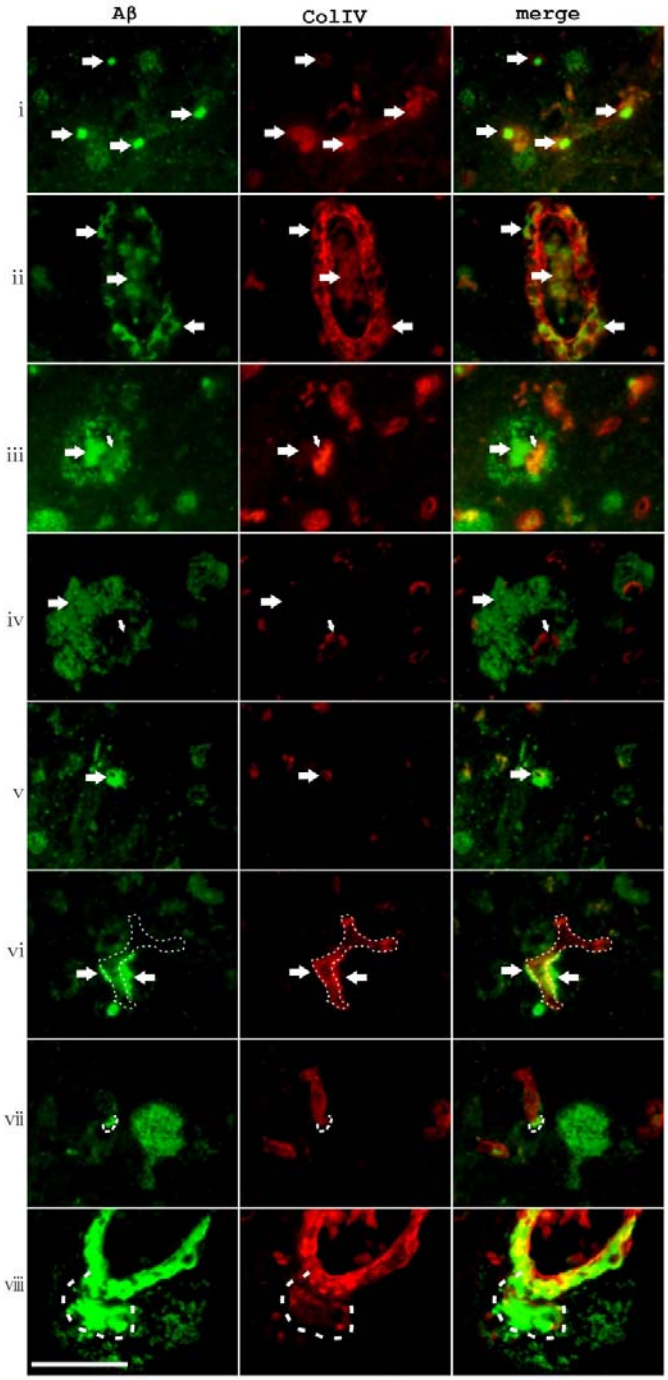

Figure 5. **The dynamic interaction of Aβ expression and blood vessels in senile plaque development.** (i) Discrete condensed Aβ staining was observed in the blood vessels. (ii) Strong Aβ staining associated with CAA blood vessel wall and also red blood cells. (iii-iv) Dense-core or diffusive senile plaque Aβ staining associated with abnormal blood vessel morphology resembling vessel breakage. (v -vi) The leakage of Aβ out of a small capillary and a larger blood vessel was observed. (vii-viii) Bulge-like structures were observed in both small and larger blood vessels containing

concentrated Aβ, suggesting blood vessel aneurysm might be happening. Large arrows indicated Aβ stainings. Small arrows indicated abnormal openings in the blood vessel wall. Dashed lines indicated the outline of blood vessels or outlines of blood vessel aneurysm. Scale bar, 50 μm.

To further confirm that blood leakage is the primary source of senile plaque Aβ, we used another blood vessel marker LRP1 to examine the relation of Aβ and blood vessel. Not surprisingly, we also observed condensed Aβ came out of blood capillaries precisely on site through openings on the capillary wall (Figure 6A). Platelets was previously thought to be related to senile plaque formation and be a potential source of APP[20]. We used CD42b as a marker of platelets to analyze the behavior of platelets during senile plaque formation. We found that Aβ-positive and CD42b-positive platelets attached to blood vessel walls, indicating the presence of blood vessel damage as it is well-known that blood vessel wall damage activates platelets and attracts platelets to the damage sites (Figure 6B(ⅰ)). Large aggregations of CD42b-positive platelets were also found in the blood vessels, suggesting the happening of intravascular coagulation events (Figure 6B(ⅱ)). Additionally, CD42b-positive platelets were found in dense-core senile plaques (Figure 6B(ⅲ)). However, the staining of Aβ on platelets was in general lower comparing to what we observed in the red blood cells (Supplementary Figure 2). With complicated regulations between platelets and blood cells [21-24], platelet could be another significant player involving blood leakage and senile plaque formation besides red blood cells.

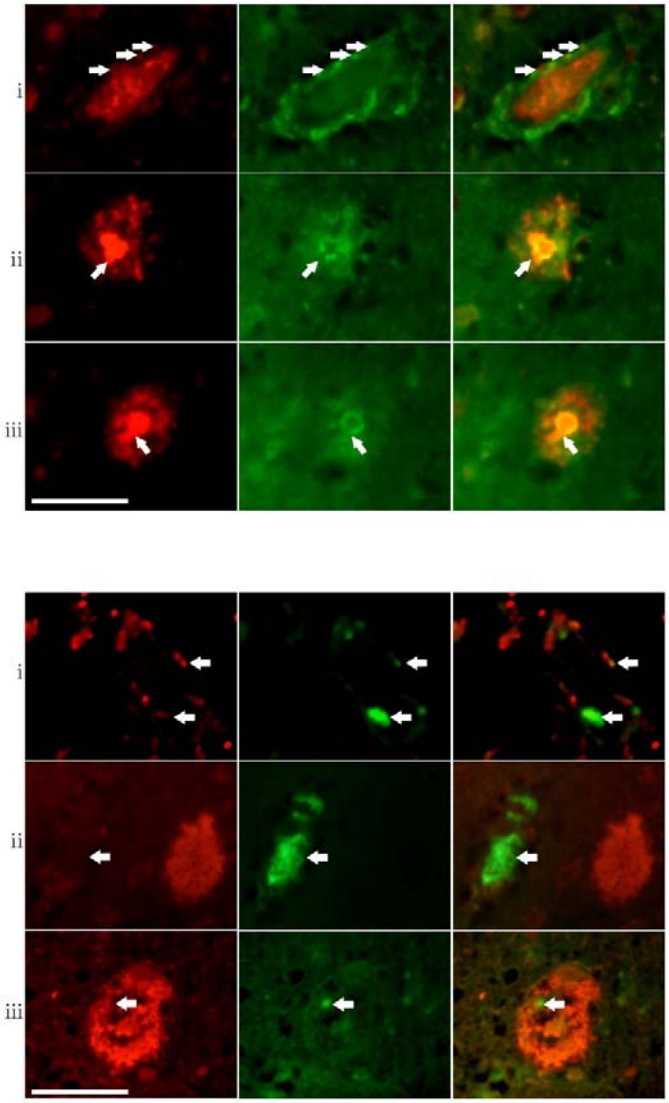

Figure 6. **Co-immunostaining of blood vessel marker LRP1 and platelet marker CD42b with Aβ in AD tissues. A**: The leakage of Aβ out of LRP1 labeled capillaries was directly observed. (ⅰ) LRP1 labeled cerebral blood vessel wall. (ⅱ-ⅲ) Aβ was observed to leak out of broken capillary wall openings labeled by LRP1. The arrows indicated vessel stainings and vessel openings. **B**: CD42b staining signified potential vessel damage and coagulation reactions but with relatively weak staining of Aβ in platelets. (ⅰ) Platelets marked with CD42b were attached to blood vessel wall, indicating blood vessel wall damage. (ⅱ) Aggregations of CD42b indicated intravascular platelet coagulation reaction. However, this platelet aggregation did not have a strong Aβ staining. (ⅲ) A platelet was observed in a dense-core senile plaque. The arrows indicated platelets. Scale bars, 50 μm.

Discussion

Senile plaque Aβ has been hypothesized to be derived from neural or vascular/blood source[8,12,15,25]. Platelets and red blood cells are proposed to be two main cellular sources of Aβ in the blood[26-29]. This study indicated the primary source of Aβ is not neural cells with the evidence showing a lack of substantial colocalization of senile Aβ with neural markers. The direct origin of senile plaque Aβ is likely coming from red blood cell-associated Aβ leakage out of damaged blood vessels. The evidence is the following: First, red blood cells in AD patients were stained with Aβ antibody strongly. Second, Aβ is colocalized with red blood cell markers such as HBA and and plasma marker ApoE at multiple stages of senile plaque development such as CAA, dense-core plaques and diffusive plaques. The colocalization of Hemoglobin and Aβ in the senile plaques has previously been reported by another research group[28,29]. Thirdly, senile plaques contained a characteristic blue fluorescence from materials named as MetaBlue, which is also predominantly localized in the blood stream. MetaBlue colocalized with red blood cells and also appeared in the CAA vessel walls and in the senile plaques similarly as Aβ. Finally, direct leakage of Aβ out of cerebral capillary openings upon capillary wall damage was observed using both Collagen IV and LRP1 as blood vessel markers. Although our pathology analysis only provided static images of related events, since the blood vessels are constantly under blood pressure, vascular damage very likely leads to unidirectional blood content leakage out of blood vessel into brain parenchyma. It is hard to imagine that things go with the opposite direction in which neuronal brain parenchyma Aβ accumulation results vascular openings and inward flow of concentrated Aβ into the blood stream against blood pressure influence. However, a negative impact of high intravascular Aβ level on blood cell physiology or vascular endothelial cell connectivity is possible. Under normal physiological conditions, Aβ and other metabolic waste-associated molecules could be accumulated in the blood stream against the metabolic waste concentration gradient by active transcellular transport through glial cells, vascular smooth muscle cells and endothelial cell networks. However, this metabolic waste transport and

accumulation process is interrupted and reversed with the blood vessel integrity being compromised, which results the reverse spill of blood-borne Aβ into the brain parenchyma. In summary, our data suggested that senile plaque formation is primarily induced by red blood cell leakage along with the leakage of other blood contents.

Platelets have been suggested as an important source of APP in the blood stream that contributes to plasma Aβ[20,30]. Our experiment showed that, although CD42b-positive platelets are stained weakly positive for Aβ in the blood vessels, on the blood vessel walls or even inside of amyloid plaques, the contribution of platelet Aβ to senile plaque formation is less than the contribution of red blood cell Aβ (Figure 6 and Supplementary Figure 2). Since it was previously reported that platelets release APP in alpha-granules after platelet activation[31,32]. It is possible that some of Aβ that associated with red blood cells were actually derived from platelet cells. MetaBlue fluorescent signals also showed that the bulk of blue autofluorescence material is associated with red blood cells but not platelets (Supplementary Figure 2). All these data suggested that red blood cells leakage is the primary starting point of senile plaque formation, with additional involvement of platelets, and a variety of blood-borne materials such as ApoE and MetaBlue.

This study analyzed several neural markers such as MAP2, αSYN, phos-Tau, GFAP, and Iba1 in senile plaques. We found some colocalizations of glial markers with senile plaque Aβ but overall few colocalizations of neuronal markers with senile plaque Aβ. This suggested that neurons are not likely the direct source of senile plaque Aβ. In addition, TUNEL assay showed that neurons not necessarily have high positive ratio of strong TUNEL labeling comparing to other cell types such as glia and blood vessel smooth muscle cells and endothelial cells (Supplementary Figure 3). Among the top 20% high intensity TUNEL stained cells analyzed in AD brain tissues, neurons, astrocytes and microglial cells each account for approximately 12%, while other cell types account for around 64% of the high intensity cells. Further, using gastric cancer tissues with abundant TUNEL-positive dying cells as TUNEL-positive cell death

tissue controls，our experiment suggested that TUNEL-labeling in AD brains is significantly weaker than TUNEL-labeling of dying cells in gastric cancer tissues. The average TUNEL intensity of top 20% highly intensive TUNEL-labeled AD brain cells is around 26% of TUNEL-labeling intensity of dying cells in gastric cancer tissues (Supplementary Figure 4). Similarly，a previous study in AD mouse models only detected 0.4% neurons might undergo oxidative-stress related cell death[33]. In our own analysis, the most intensive 2 out of 60 randomly-selected cells in AD tissues reached around 50% of the average TUNEL intensity of the dying cells in gastric cancer tissues, suggesting a very low true dying cell number in AD tissues. As it is well-known, TUNEL assay not only labels apoptotic cells but also labels DNA damage. It is very likely that the relatively low intensity of TUNEL labeling in AD tissues reflects DNA damage instead of cell apoptosis. AD tissues might not have abundant neuronal cell death as people previously thought. Moreover, we analyzed general oxidative stress or proteostatic stress markers in AD tissues and found blood vessel associated cells have stronger staining of MDA (Malondialdehyde), LC3, Lamp2, and UBB comparing to the staining in senile plaques. All together, our study indicated that the blood vessel components in AD tissues are under a high metabolic stress pressure (Supplementary Figure 5). The exact functions of neural involvement in senile plaques need to be further investigated, which likely associated with blood leakage material clearance and damage control over proteostatic, metabolic or inflammatory insults after cerebral microhemorrhage and microaneurysm. Neural involvement in managing cerebral vessel leakage is likely an active process, and Tau phosphorylation might be linked to the blood material clearance. In review of the literature, we agree that AD is a vascular disease with neurological consequences, which was strongly proposed by Dr. de la Torre, Dr. Stone， Dr. Miyakawa and others[9,27,34-36].

Among different vascular abnormalities, CAA has long been linked with AD development[2,37-40]. This study suggested that CAA could be an important intermediate step during the blood leakage process. The blood leakage likely helps to temporarily

release the metabolic pressure inside of CAA blood vessels, which benefits subsequent blood vessel repair and the survival of affected individuals. The reason of the coexisting of CAA vessels and non-CAA vessels in a single AD patient is because that condensed Aβ only transiently associated with vessel walls and the vessels will have low amyloid load after amyloid-associated blood contents leaking out of blood vessel through either direct leakage or microaneurysm formation.

The findings that senile plaques are associated with specific blue autofluorescence are intriguing. There have been a number of studies related to senile plaque blue autofluorescence materials in the past[17,18,41]. To facilitate the study on this potential important blue fluorescent material, we named it as MetaBlue in this article. An early study reported that the blue autofluorescence was associated with senile plaques but not CAA[17]. Two more recent studies found that the blue autofluorescence was associated with both senile plaques and CAA[18,41]. Our study additionally found that MetaBlue was not only associated with senile plaques and CAA but also directly associated with red blood cells in the blood stream. Our preliminary data indicated that MetaBlue also exists in the blood stream of normal brain tissue samples so that it does not uniquely exist in AD patients. The exact identity of MetaBlue is unknown. MetaBlue could be an oxidative-stress related metabolite since previous literature indicated that blue autofluorescence of amyloid peptides could be associated with tyrosine oxidation[42]. To isolate MetaBlue materials and to elucidate the true identity of MetaBlue will likely leads to deep understanding of AD pathogenesis.

Material and methods

Tissue sections. AD tissue sections were purchased from GeneTex (Irvine, CA, USA). Additionally, AD tissue sections were provided by National Human Brain Bank for Development and Function, Chinese Academy of Medical Sciences and Peking Union Medical College, Beijing, China. This study was supported by the Institute of Basic Medical Sciences, Chinese Academy of Medical Sciences, Neuroscience Center, and

the China Human Brain Banking Consortium. Gastric cancer tissues as TUNEL assay positive controls were purchased from Shanghai ENOVO Industrial Co.

List of antibodies for immunocytochemistry. The following primary antibodies and dilutions have been used in this study: MDA (Abcam ab6463, 1:200), UBB (Proteintech 10201-2-AP, 1:200), Lamp2 (Proteintech 66301-1-Ig, 1:100), LC3 (This antibody detects both LC3A and LC3B) (Proteintech 66139-1-Ig, 1:500), phos-TAU (Abcam ab151559, 1:200), Aβ (Abcam ab201061, 1:200), Aβ/APP (CST #2450, 1:200) , ColIV（Abcam ab236640， 1:200）, LRP1 （Abcam ab92544， 1:200） , ApoE （Abcam ab183597， 1:200）, CD42b （Abcam ab210407， 1:200）, HBA （Abcam ab92492， 1:200）, GFAP （Abcam ab33922， 1:200）, Iba1 （Abcam ab178847， 1:200）, αSyn (Proteintech 10842-1-AP, 1:200). The following secondary antibodies and dilutions have been used in this study: donkey anti-mouse Alexa 594nm secondary antibody (Jackson ImmunoResearch 715-585-150, 1:400) , donkey anti-rabbit Alexa-488nm secondary antibody (Jackson ImmunoResearch 711-545-152, 1:400) , donkey anti-rabbit Alexa 594nm secondary antibody (Jackson ImmunoResearch 711-585-152, 1:400) , donkey anti-mouse Alexa-488nm secondary antibody (Jackson ImmunoResearch 715-545-150, 1:400).

Immunocytochemistry was performed as described[43]. Briefly, paraffin sections were deparaffinized by Xylene, 100% EtOH, 95% EtOH, 75% EtOH, 50% EtOH, and PBS washes. Sections were treated with 10 mM pH6.0 sodium citrate or 10mM pH9.0 Tris-EDTA solution with microwave at high power for 3 times of 4 minutes, with 5 minutes intervals. The sections were allowed to naturally cool down to room temperature. Then, the slides were blocked with TBST 3%BSA solution for 1 hour at room temperature. After blocking, the samples were incubated with primary antibodies at room temperature for 2 hrs followed by 5 washes of TBST. After that, the samples were incubated with fluorescent secondary antibodies overnight at 4 degrees. The treated samples were washed again with TBST 5 times the second day

and mounted with PBS+50% glycerol supplemented with H33342 nuclear dye (Sigma, B2261，1 μg/ml) and ready for imaging. To differentiate nuclear staining from MetaBlue autofluorescence signal, in some of the IHC experiments, PI (Sigma, P4170, 10 μg/ml) was used as a red nuclear fluorescence dye instead of H33342, which stained the nuclei with blue fluorescence. IHC experiments without primary antibodies were used as negative controls. All experiments have been repeated in order to verify the reproducibility of the results.

TUNEL assay. TUNEL assay kits were purchased from Beyotime Biotechnology (Shanghai, China). TUNEL assay was performed as described in the manufacturer's user manual. Briefly, paraffin sections were deparaffinized by Xylene, 100% EtOH, 95% EtOH, 75% EtOH, 50% EtOH, and ddH_2O washes. Then, the sections were digested with Proteinase K (20μg/ml) in 10mM TE buffer (pH 7.5) for 15 minutes at room temperature. After Proteinase K digestion, the slides were washed with PBS for 5 times. The slides were then incubated in 50μl freshly-prepared TUNEL labeling mixture, covered with parafilm and incubated for 1 hour at 37 degree. Afterwards, the slides were washed with PBS for 5 times and mounted with 50% Glycerol/PBS solution with Hoechst nuclear dye and examined under fluorescent microscopes. To perform double labeling of TUNEL and antibody staining, the incubation time of Proteinase K treatment was shortened and adjusted to allow the simultaneous detection of protein antigens and TUNEL signals. When performing TUNEL labeling intensity comparisons with positive TUNEL controls, identical experiment procedure was used for different tissue samples.

I**maging and morphometry analysis**. All images were taken with a Leica DM6000B microscope (Leica Microsystems, Wetzlar, Germany) with A4, L5 and N3 fluorescent filter cubes. The microscope is equipped with 10X eyepiece, and 5X, 10X, 20X, 40X objective lens and 1.6X digital zoom. When comparing marker immunostaining densities, identical exposure settings for fluorescent channels were used for both control and test groups. Images were then analyzed with Lecia Advanced

Fluorescence software or ImageJ software. Average area density was used as the parameter to define the marker densities. For TUNEL staining intensity comparison, approximately 60 control TUNEL positive dying cells in processed gastric cancer tissues were first measured with the software and the average value was used as the control value. 60 TUNEL-labeled cells in AD tissues were measured with software and the obtained values divide the control value to obtain the values of fold of changes. The folds of changes were then expressed as means with standard deviations.

Statistics. All data first went through a Shapiro & Wilk normality test using SPSS Statistics 19 software. Two-tailed unpaired T-test was used to compare the means of data with a normal distribution with Excel 2007 software. For data that were not normally distributed, nonparametric Mann/Whitney test was performed to compare the means with Megastat addin version 10.2. The p Value threshold for statistical significance is set at 0.05. If $p<0.05$, then the difference was considered statistically significant. When $p<0.001$, it was labeled as $p<0.001$. If $p \geqq 0.001$, then the p Value was shown as it was. "*" in the statistical figures indicated the differences are statistically significant.

Data and materials availability. All data needed to evaluate the conclusions in this paper are present either in the main text or the supplementary materials.

Supplementary Materials.

Supplementary Figs. 1-5

Acknowledgements: We thank Housheng Wang, Lu Xu, Wenting Xuan, Pingxin Liu, Xiaoyi Bao, Jun Wang for excellent lab assistance. **Funding**: This work was supported by National Natural Science Foundation of China No. 81472235 (H.F.), Shanghai Jiao Tong University Research Grant YG2017MS71 (D.P. and H.F.). **Author contributions:** H.F. conceived the study; H. F. designed and supervised the

experiments; H.F. and J. L. performed the experiments; H. F., J. L., D.P., W. J., D. C. did the data analysis; H. F. wrote the manuscript; All authors reviewed the manuscript.

Competing interests: Authors declare no competing interests.

References:

1 Lane, C. A., Hardy, J. & Schott, J. M. Alzheimer's disease. *Eur J Neurol* **25**, 59-70, doi:10.1111/ene.13439 (2018).

2 Attems, J., Lintner, F. & Jellinger, K. A. Amyloid beta peptide 1-42 highly correlates with capillary cerebral amyloid angiopathy and Alzheimer disease pathology. *Acta neuropathologica* **107**, 283-291, doi:10.1007/s00401-004-0822-6 (2004).

3 van Helmond, Z., Miners, J. S., Kehoe, P. G. & Love, S. Oligomeric Abeta in Alzheimer's disease: relationship to plaque and tangle pathology, APOE genotype and cerebral amyloid angiopathy. *Brain Pathol* **20**, 468-480, doi:10.1111/j.1750-3639.2009.00321.x (2010).

4 Glenner, G. G., Henry, J. H. & Fujihara, S. Congophilic angiopathy in the pathogenesis of Alzheimer's degeneration. *Annales de pathologie* **1**, 120-129 (1981).

5 Glenner, G. G. & Wong, C. W. Alzheimer's disease: initial report of the purification and characterization of a novel cerebrovascular amyloid protein. *Biochemical and biophysical research communications* **120**, 885-890, doi:10.1016/s0006-291x(84)80190-4 (1984).

6 Masters, C. L. *et al.* Amyloid plaque core protein in Alzheimer disease and Down syndrome. *Proceedings of the National Academy of Sciences of the United States of America* **82**, 4245-4249, doi:10.1073/pnas.82.12.4245 (1985).

7 Hardy, J. Alzheimer's disease: the amyloid cascade hypothesis: an update and reappraisal. *Journal of Alzheimer's disease : JAD* **9**, 151-153, doi:10.3233/jad-2006-9s317 (2006).

8 Hardy, J. A. & Higgins, G. A. Alzheimer's disease: the amyloid cascade hypothesis. *Science* **256**, 184-185, doi:10.1126/science.1566067 (1992).

9 Miyakawa, T., Shimoji, A., Kuramoto, R. & Higuchi, Y. The relationship between senile plaques and cerebral blood vessels in Alzheimer's disease and senile dementia. Morphological mechanism of senile plaque production. *Virchows Archiv. B, Cell pathology including molecular pathology* **40**, 121-129, doi:10.1007/bf02932857 (1982).

10 Kawai, M., Kalaria, R. N., Harik, S. I. & Perry, G. The relationship of amyloid plaques to cerebral capillaries in Alzheimer's disease. *The American journal of pathology* **137**, 1435-1446 (1990).

11 Sparks, D. L., Kuo, Y. M., Roher, A., Martin, T. & Lukas, R. J. Alterations of Alzheimer's disease in the cholesterol-fed rabbit, including vascular inflammation. Preliminary observations. *Annals of the New York Academy of Sciences* **903**, 335-344, doi:10.1111/j.1749-6632.2000.tb06384.x (2000).

12 Cullen, K. M., Kocsi, Z. & Stone, J. Microvascular pathology in the aging human brain: Evidence that senile plaques are sites of microhaemorrhages. *Neurobiol Aging* **27**, 1786-1796, doi:10.1016/j.neurobiolaging.2005.10.016 (2006).

13 Kumar-Singh, S. *et al.* Dense-core senile plaques in the Flemish variant of Alzheimer's disease

are vasocentric. *The American journal of pathology* **161**, 507-520, doi:10.1016/S0002-9440(10)64207-1 (2002).

14 Kumar-Singh, S. *et al.* Dense-core plaques in Tg2576 and PSAPP mouse models of Alzheimer's disease are centered on vessel walls. *The American journal of pathology* **167**, 527-543, doi:10.1016/S0002-9440(10)62995-1 (2005).

15 Bu, X. L. *et al.* Blood-derived amyloid-beta protein induces Alzheimer's disease pathologies. *Molecular psychiatry* **23**, 1948-1956, doi:10.1038/mp.2017.204 (2018).

16 Ryu, J. K. & McLarnon, J. G. A leaky blood-brain barrier, fibrinogen infiltration and microglial reactivity in inflamed Alzheimer's disease brain. *Journal of cellular and molecular medicine* **13**, 2911-2925, doi:10.1111/j.1582-4934.2008.00434.x (2009).

17 Dowson, J. H. A sensitive method for the demonstration of senile plaques in the dementing brain. *Histopathology* **5**, 305-310, doi:10.1111/j.1365-2559.1981.tb01789.x (1981).

18 Gao, Y. *et al.* Imaging and Spectral Characteristics of Amyloid Plaque Autofluorescence in Brain Slices from the APP/PS1 Mouse Model of Alzheimer's Disease. *Neuroscience bulletin* **35**, 1126-1137, doi:10.1007/s12264-019-00393-6 (2019).

19 Scheibel, A. B. Alterations of the cerebral capillary bed in the senile dementia of Alzheimer. *The Italian Journal of Neurological Sciences* **8**, 457-463, doi:10.1007/bf02334602 (1987).

20 Li, Q. X. *et al.* Membrane-associated forms of the beta A4 amyloid protein precursor of Alzheimer's disease in human platelet and brain: surface expression on the activated human platelet. *Blood* **84**, 133-142 (1994).

21 Koupenova, M., Kehrel, B. E., Corkrey, H. A. & Freedman, J. E. Thrombosis and platelets: an update. *European heart journal* **38**, 785-791, doi:10.1093/eurheartj/ehw550 (2017).

22 Ferguson, D. J. Acute intravascular hemolysis after a platelet transfusion. *CMAJ : Canadian Medical Association journal = journal de l'Association medicale canadienne* **138**, 523-524 (1988).

23 Weinstein, L. Syndrome of hemolysis, elevated liver enzymes, and low platelet count: A severe consequence of hypertension in pregnancy. *Am J Obstet Gynecol* **193**, 859-860, doi:10.1016/j.ajog.2005.02.113 (2005).

24 Helms, C. C. *et al.* Mechanisms of hemolysis-associated platelet activation. *Journal of Thrombosis and Haemostasis* **11**, 2148-2154, doi:10.1111/jth.12422 (2013).

25 de la Torre, J. C. & Aliev, G. Alzheimer's disease is a vascular disorder with neurodegenerative consequences. *J Neurol Sci* **229**, 305-306 (2005).

26 Humpel, C. Platelets: Their Potential Contribution to the Generation of Beta-amyloid Plaques in Alzheimer's Disease. *Curr Neurovasc Res* **14**, 290-298, doi:10.2174/1567202614666170705150535 (2017).

27 Stone, J. What initiates the formation of senile plaques? The origin of Alzheimer-like dementias in capillary haemorrhages. *Medical hypotheses* **71**, 347-359, doi:10.1016/j.mehy.2008.04.007 (2008).

28 Chuang, J. Y. *et al.* Interactions between amyloid-beta and hemoglobin: implications for amyloid plaque formation in Alzheimer's disease. *PloS one* **7**, e33120, doi:10.1371/journal.pone.0033120 (2012).

29 Wu, C. W. *et al.* Hemoglobin promotes Abeta oligomer formation and localizes in neurons and amyloid deposits. *Neurobiology of disease* **17**, 367-377, doi:10.1016/j.nbd.2004.08.014 (2004).

30 Canobbio, I. *et al.* Platelet amyloid precursor protein is a modulator of venous thromboembolism in mice. *Blood* **130**, 527-536, doi:10.1182/blood-2017-01-764910 (2017).

31 Smith, R. P. & Broze, G. J., Jr. Characterization of platelet-releasable forms of beta-amyloid precursor proteins: the effect of thrombin. *Blood* **80**, 2252-2260 (1992).

32 Van Nostrand, W. E., Schmaier, A. H., Farrow, J. S. & Cunningham, D. D. Platelet protease nexin-2/amyloid beta-protein precursor. Possible pathologic and physiologic functions. *Annals of the New York Academy of Sciences* **640**, 140-144, doi:10.1111/j.1749-6632.1991.tb00205.x (1991).

33 Xie, H. *et al.* Rapid cell death is preceded by amyloid plaque-mediated oxidative stress. *Proceedings of the National Academy of Sciences of the United States of America* **110**, 7904-7909, doi:10.1073/pnas.1217938110 (2013).

34 de la Torre, J. C. Is Alzheimer's disease a neurodegenerative or a vascular disorder? Data, dogma, and dialectics. *Lancet Neurol* **3**, 184-190, doi:Doi 10.1016/S1474-4422(04)00683-0 (2004).

35 De La Torre, J. C. Vascular basis of Alzheimer's pathogenesis. *Ann Ny Acad Sci* **977**, 196-215 (2002).

36 Miyakawa, T. Vascular pathology in Alzheimer's disease. *Psychogeriatrics : the official journal of the Japanese Psychogeriatric Society* **10**, 39-44, doi:10.1111/j.1479-8301.2009.00294.x (2010).

37 Joachim, C. L., Mori, H. & Selkoe, D. J. Amyloid β-protein deposition in tissues other than brain in Alzheimer's disease. *Nature* **341**, 226-230, doi:10.1038/341226a0 (1989).

38 Attems, J., Yamaguchi, H., Saido, T. C. & Thal, D. R. Capillary CAA and perivascular A beta-deposition: Two distinct features of Alzheimer's disease pathology. *J Neurol Sci* **299**, 155-162, doi:10.1016/j.jns.2010.08.030 (2010).

39 Vinters, H. V. & Gilbert, J. J. Cerebral amyloid angiopathy: incidence and complications in the aging brain. II. The distribution of amyloid vascular changes. *Stroke* **14**, 924-928, doi:10.1161/01.str.14.6.924 (1983).

40 Vidoni, E. D. *et al.* Cerebral beta-Amyloid Angiopathy Is Associated with Earlier Dementia Onset in Alzheimer's Disease. *Neurodegener Dis* **16**, 218-224, doi:10.1159/000441919 (2016).

41 Kwan, A. C., Duff, K., Gouras, G. K. & Webb, W. W. Optical visualization of Alzheimer's pathology via multiphoton-excited intrinsic fluorescence and second harmonic generation. *Opt Express* **17**, 3679-3689, doi:10.1364/Oe.17.003679 (2009).

42 Fricano, A., Librizzi, F., Rao, E., Alfano, C. & Vetri, V. Blue autofluorescence in protein aggregates "lighted on" by UV induced oxidation. *Biochimica et biophysica acta. Proteins and proteomics* **1867**, 140258, doi:10.1016/j.bbapap.2019.07.011 (2019).

43 Fu, H. *et al.* Persisting and Increasing Neutrophil Infiltration Associates with Gastric Carcinogenesis and E-cadherin Downregulation. *Scientific reports* **6**, 29762, doi:10.1038/srep29762 (2016).

Supplementary Information for

Senile plaques in Alzheimer's disease are primarily induced by cerebral vessel leakage of red blood cells and other blood contents

Hualin Fu, Jilong Li, Peng Du, Weilin Jin, Daxiang Cui

This PDF file includes:

Supplementary Fig. 1 to 5

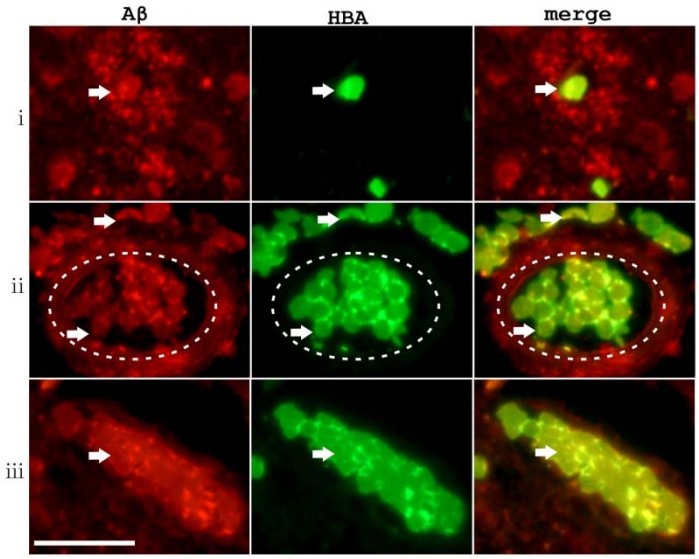

Supplementary Figure 1. **The colocalization of Aβ and red blood cell alpha Hemoglobin （HBA）.** (i) Aβ staining of a single red blood cell marked with HBA in the center of a senile plaque. (ii) Aβ staining of red blood cells marked with HBA during red blood cell extravasation. (iii) Aβ staining of red blood cells marked with HBA during intravascular hemolysis with the disappearance of clear round shape structure of red blood cells. The arrow indicated Aβ and HBA co-staining. The dashed lines in (ii) indicated the outline of a blood vessel. Scale bar, 50 μm.

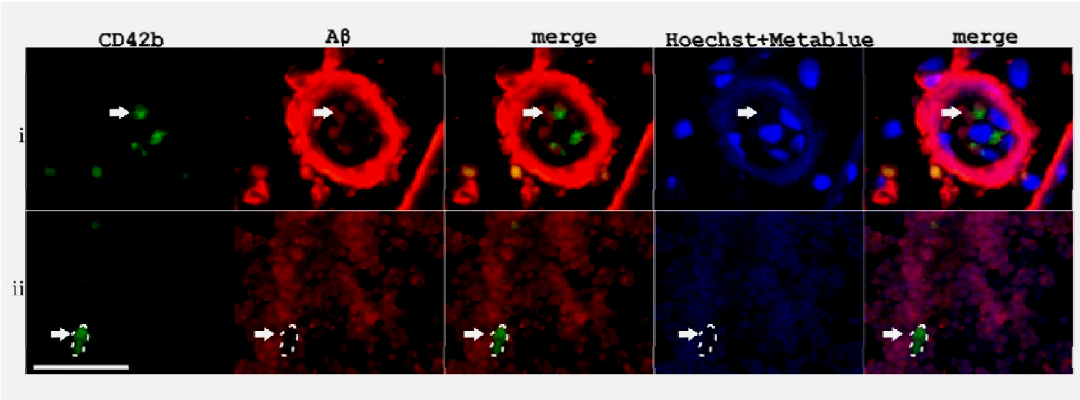

Supplementary Figure 2. **Aβ or MetaBlue is mostly associated with red blood cells but not platelets.** (i) Platelets induced small red cell cluster formation in the blood vessel. (ii) Most Aβ or MetaBlue staining was associated with red blood cells instead of platelets marked by CD42b. The arrows indicated red blood cells. The dashed line indicated platelet aggregation. Scale bar, 50 μm.

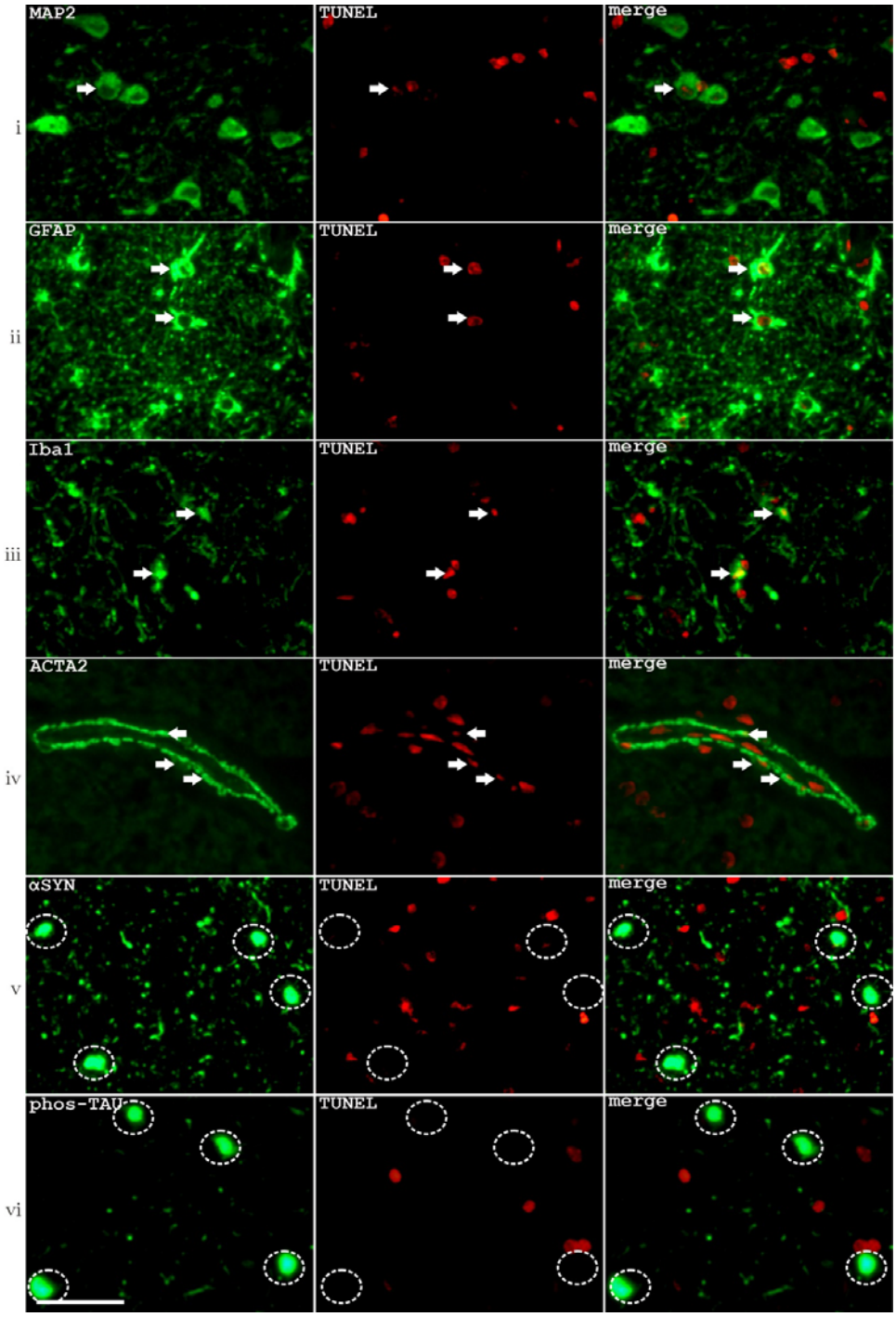

Supplementary Figure 3. Neurons, astral glia cells, microglial cells, neurofibillary tangles or Lewy bodies (in green) were not particularly associated with high intensity of TUNEL labeling and blood vessels have significant TUNEL staining. (ⅰ) MAP2 (neuron marker); (ⅱ) GFAP (astrocyte marker); (ⅲ) Iba1 (microglial marker); (ⅳ) ACTA2 (blood vessel marker); (ⅴ) αSYN; (ⅵ) phos-Tau. The arrows indicated TUNEL-positive cells. The dashed circles indicated Lewy

bodies or Tau-tangles. Scale bar, 50 μm.

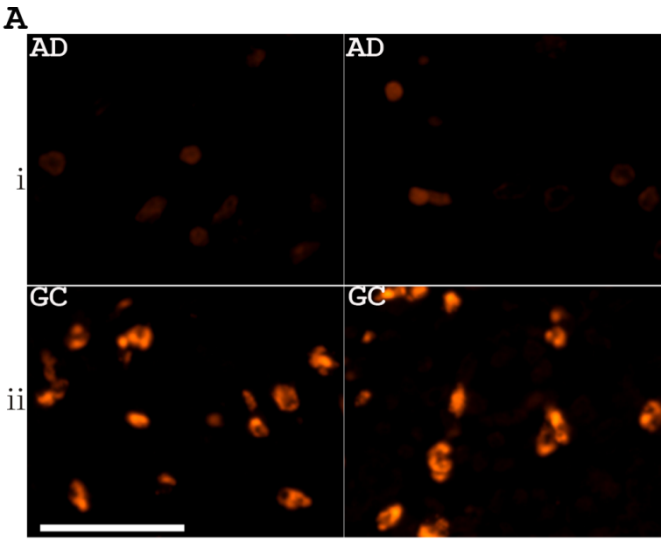

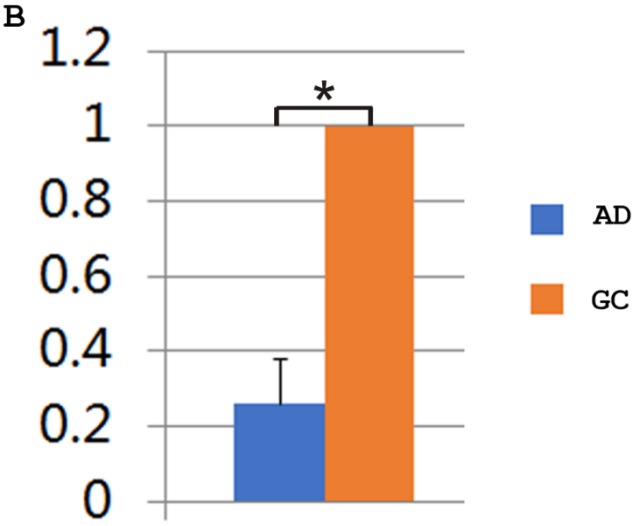

Supplementary Figure 4. **The intensity of TUNEL labeling in AD tissues is significantly lower than dying cells in GC tissues.** **A**: TUNEL staining of AD tissues was compared with TUNEL labeling in gastric cancer tissues (GC). Scale bar, 50 μm. **B**: The average TUNEL intensity of AD tissue cells was significantly lower than TUNEL labeling intensity of dying cells in gastric cancer tissues (0.26±0.12, $p<0.001$).

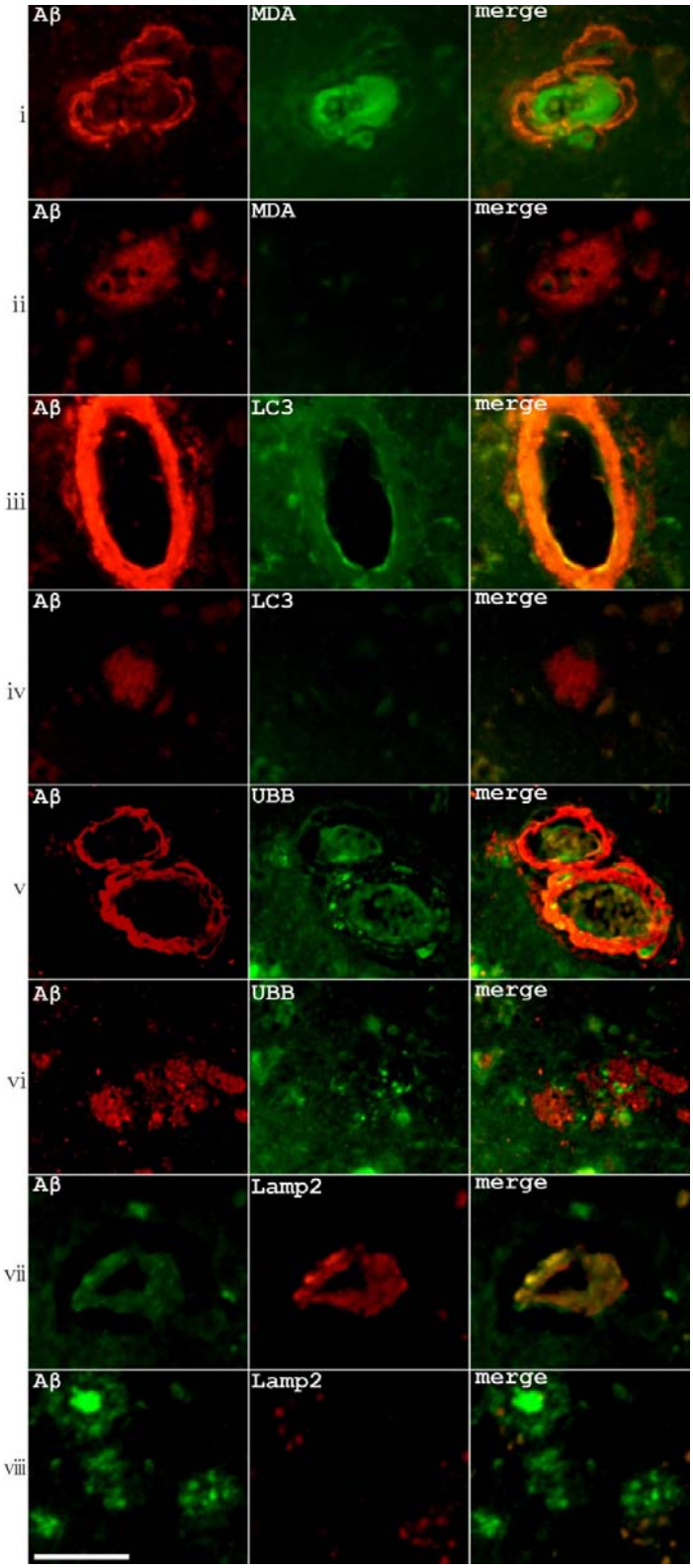

Supplementary Figure 5. AD blood vessels (ⅰ, ⅲ, ⅴ, ⅶ) have generally stronger expression of metabolic stress markers such as MDA, LC3, UBB and Lamp2 comparing to senile plaques (ⅱ, ⅳ, ⅵ, ⅷ). Scale bar, 50 μm.